

## Electrocatalytic Determination of Cysteamine Using Multiwall Carbon Nanotube Paste Electrode in the Presence of 3,4-Dihydroxycinnamic Acid as a Homogeneous Mediator

Mohsen Keyvanfard,<sup>\*a</sup> Samad Sami,<sup>b</sup> Hassan Karimi-Maleh<sup>a</sup> and Khadijeh Alizad<sup>a</sup>

<sup>a</sup>Department of Chemistry, Majlesi Branch, Islamic Azad University, Isfahan, Iran

<sup>b</sup>Department of Chemistry, Shahreza Branch, Islamic Azad University, Isfahan, Iran

A eletrooxidação da cisteamina (CA) foi estudada por eletrodos de pasta de nanotubos de carbono modificados com ácido 3,4-di-hidroxicinnâmico (3,4-DHCA) usando voltametria cíclica, cronoamperometria e voltametria de varredura linear. Usando o eletrodo modificado, a cinética de eletrooxidação da CA foi consideravelmente intensificada através da redução do potencial anódico por meio de uma reação catalítica. O mecanismo de comportamento eletroquímico da CA na superfície do eletrodo modificado foi analisado por vários métodos eletroquímicos, na presença de mediador. O eletrodo modificado preparado apresentou respostas voltamétricas com alta sensibilidade para CA, o que o torna muito adequado para a detecção de CA em quantidades de traço. Um intervalo dinâmico linear de 0,25-400  $\mu\text{mol L}^{-1}$  para a CA foi obtida em solução tamponada com pH 7,0. O limite de detecção foi de 0,09  $\mu\text{mol L}^{-1}$ .

The electrooxidation of cysteamine (CA) was studied by modified carbon nanotubes paste electrode in the presence of 3,4-dihydroxycinnamic acid (3,4-DHCA) using cyclic voltammetry, chronoamperometry and linear sweep voltammetry. Using the modified electrode, the kinetics of CA electrooxidation was considerably enhanced by lowering the anodic over-potential through a catalytic fashion. The mechanism of CA electrochemical behavior at the modified electrode surface was analyzed by various electrochemical methods in the presence of mediator. The prepared modified electrode showed voltammetric responses with high sensitivity for CA, making it very suitable for the detection of CA at trace levels. A linear dynamic range of 0.25-400  $\mu\text{mol L}^{-1}$  for CA was obtained in buffered solutions with pH 7.0. The limit of detection was 0.09  $\mu\text{mol L}^{-1}$ .

**Keywords:** cysteamine, electrocatalysis, voltammetry, multiwall carbon nanotubes, 3,4-dihydroxycinnamic acid

### Introduction

Cysteamine is an important thiol drug for the treatment of cystinosis.<sup>1</sup> The deficiency of a cystine carrier in the lysosomal membrane leads to cystine accumulation within the lysosomes, ultimately crystallizing in vital organs such as the liver, kidney, spleen, intestines, and cornea.<sup>2,3</sup> A number of long term clinical trials have shown that cysteamine administration (as cysteamine hydrochloride) stabilizes renal function, delays glomerular deterioration and improves linear growth.<sup>4</sup> Cysteamine and its disulfide, cystamine, have been shown to be neuroprotective in a number of cell culture and animal models.<sup>5</sup> With this goal in mind, a rapid but specific and sufficiently sensitive analytical method was required for total cysteamine determination in biological and pharmaceutical samples. Numerous methods have been reported for the

determination of CA in pharmaceutical and biological samples including chromatography,<sup>6-8</sup> electrophoresis,<sup>9</sup> gas chromatography with flame photometric detection,<sup>10</sup> ion exchange chromatography,<sup>11</sup> and electrochemical methods<sup>12-14</sup> using modified electrodes. Due to problems in chromatographic methods such as selecting a suitable column or a mobile phase with liquid chromatographic methods, long response time, expensive instruments, complicated procedure, and low detection capability<sup>15-17</sup>, electrochemical techniques for determination of CA was used in this work.

Carbon nanotubes (CNTs) are presently in the forefront of materials research in electrochemical and other fields. They are recognized as a new class of nano-materials that have had a profound impact on a wide range of applications. Carbon nanotubes have confirmed their advantages in electrochemistry and electroanalysis of some important environmental and biological compounds.<sup>18-22</sup> Hundreds

\*e-mail: keyvan45638@yahoo.com

of research articles published in recent years report many remarkable claims about the advantages of carbon nanotubes, such as increased voltammetric currents,<sup>23-25</sup> increased heterogeneous electron-transfer rates,<sup>26</sup> insignificant surface fouling of CNT-based electrodes,<sup>27,28</sup> and an apparent “electrocatalytic” effect towards the redox process of a wide variety of compounds.<sup>29-33</sup>

In this study, it was described initially the application of 3,4-dihydroxycinnamic acid as a suitable mediator in the electrocatalysis and voltammetric determination of CA in an aqueous buffer solution. In sequence, in order to demonstrate the catalytic ability of the modified electrode in the electrooxidation of CA in real samples, the method was employed for the voltammetric determination of CA in urine samples from both patients in CA treatment and healthy subjects and on medicines.

## Experimental

### Reagents and apparatus

All chemicals used were of analytical reagent grade purchased from Merck (Darmstadt, Germany) unless otherwise stated. Doubly distilled water was used throughout. Cysteamine was used from Merck.

Cysteamine solution,  $1.0 \times 10^{-3}$  mol L<sup>-1</sup>, was prepared daily by dissolving 0.008 g cysteamine in water and the solution was diluted to 100 mL with water in a 100 mL volumetric flask. The solution was kept in a refrigerator at 4 °C, in the dark. More dilute solutions were prepared by serial dilutions with water.

Phosphate buffer solutions (sodium dihydrogen phosphate and disodium monohydrogen phosphate plus sodium hydroxide, 0.1 mol L<sup>-1</sup>) with different pH values were used.

Spectrally pure graphite powder (particle size < 50 μm) from Merck and multiwall carbon nanotubes (> 90%, MWCNTs,  $d \times l = (90-70 \text{ nm}) \times (5-9 \text{ μm})$ ) from Fluka were used as the substrate for the preparation of the carbon paste electrode. High viscosity paraffin ( $d = 0.88 \text{ kg L}^{-1}$ ) from Merck was used as the pasting liquid for the preparation of the paste electrodes.

All the voltammetric measurements were performed using an Autolab PGSTAT 302N, potentiostat/galvanostat (Utrecht, The Netherlands) connected to a three-electrode cell, Metrohm (Herisau, Switzerland) Model 663 VA stand, linked with a computer (Pentium IV, 1,200 MHz) and with Autolab software. A platinum wire was used as the auxiliary electrode. Multiwall carbon nanotube paste electrode (MWCNTPE) and Ag/AgCl/KCl<sub>sat</sub> were used as the working and reference electrodes, respectively.

The electrode prepared with carbon nanotubes was characterized by scanning electron microscopy (SEM) (Seron Tech. AIS 2100). A digital pH/mV-meter (Metrohm model 710) was applied for pH measurements.

### Preparation of the electrode

To eliminate any metal oxide catalysts within the nanotubes, multiwall carbon nanotubes were refluxed in 2.0 mol L<sup>-1</sup> HNO<sub>3</sub> for 12 h, and then washed with twice-distilled water and dried at room temperature. To obtain the best conditions in the preparation of the modified electrode, the ratio of MWCNTs was optimized. The results showed that the best cyclic voltammogram (CV) shape and current was achieved with 10.0% (m/m) MWCNTs and 90.0% (m/m) graphite.

According to the above points, graphite powder (0.900 g) was dissolved in diethyl ether and hand mixed with 0.100 g carbon nanotubes with a mortar and pestle. The solvent was evaporated by stirring. A syringe was used to add paraffin to the mixture, which was mixed well for 40 min until a uniformly wetted paste was obtained. The paste was then packed into a glass tube. Electrical contact was made by pushing a copper wire down the glass tube into the back of the mixture. When necessary, a new surface was obtained by pushing an excess of the paste out of the tube and polishing it on a weighing paper.

### Preparation of real samples

Urine samples were stored in a refrigerator immediately after collection. Ten milliliters of the sample were centrifuged for 15 min at 3000 rpm. The supernatant was diluted 10 times with a phosphate buffer solution (PBS) (pH 7.0). The solution was transferred into the voltammetric cell to be analyzed without any further pretreatment. The standard addition method was used for the determination of CA in real samples.

Five capsules of cystagone 150 mg, produced by Mylan Drug Company were completely ground and homogenized. Then, 10 mg of the powder was accurately weighed and dissolved with ultrasonication in 100 mL of ethanol-water (1:2) solution. Different amounts of the solution plus 10 mL of 0.10 mol L<sup>-1</sup> buffer (pH 7.0) were used for analysis.

## Results and Discussion

### SEM characterization

Figure 1 shows SEM images for MWCNTPE and carbon paste electrode (CPE). The images show that, at the

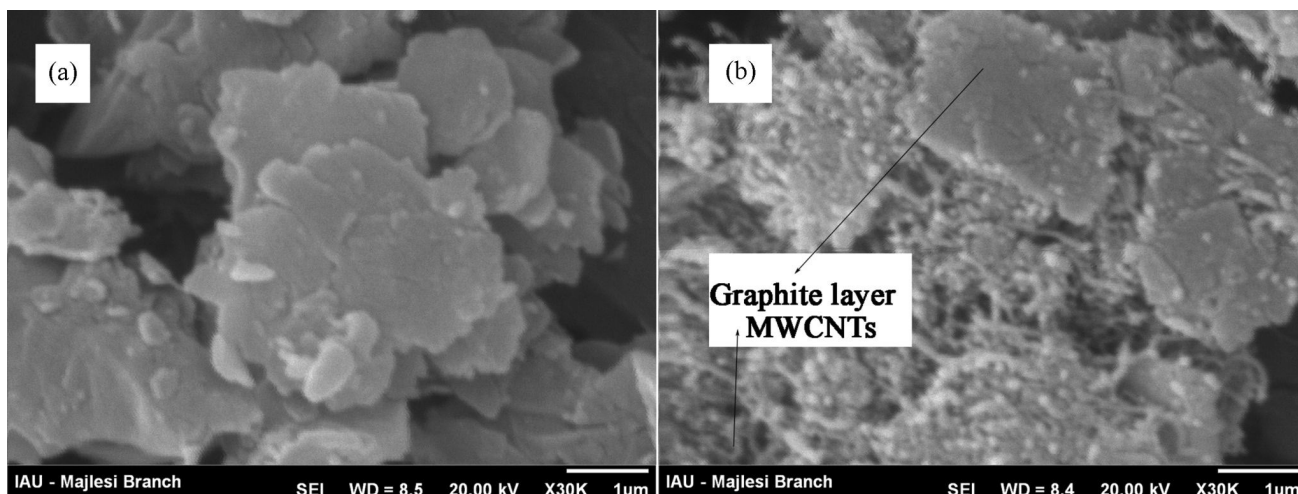


Figure 1. SEM images of (a) CPE and (b) MWCNTPE.

surface of CPE (Figure 1a), a layer of irregular flakes of graphite powder was present and isolated from each other. After multiwall carbon nanotubes (MWCNTs) were added to the carbon paste matrix, it can be seen that MWCNTs were distributed on the surface of electrode with special three-dimensional structure (Figure 1b), indicating that the MWCNTs were successfully modified on the MWCNTPE.

#### Electrochemistry of 3,4-dihydroxycinnamic acid (3,4-DHCA)

The electrochemical behavior of the 3,4-DHCA was characterized by cyclic voltmetry. Figure 2 (inset) shows the cyclic voltammograms of 3,4-DHCA at MWCNTPE in the PBS (pH 7.0) at various scan rates.

The experimental results showed well defined and reproducible anodic and cathodic peaks related to the 3,4-DHCA<sub>(red)</sub>/3,4-DHCA<sub>(ox)</sub> redox couple with a quasi reversible behavior and with a peak separation potential of  $\Delta E_p$  ( $E_{pa} - E_{pc}$ ) = 95 mV. These cyclic voltammograms were used to examine the variation of the peak currents versus the square root of potential scan rates. The plot of the anodic peak current was linearly dependent on  $v^{1/2}$  with a correlation coefficient of 0.9943 at all scan rates (Figure 2).

The active surface areas of the modified electrodes are estimated according to the slope of the  $I_p$  versus  $v^{1/2}$  plot for a known concentration of  $K_2Fe(CN)_6$ , based on the Randles-Sevcik equation,

$$I_p = 2.69 \times 105n^{3/2}A D_R^{1/2} v^{1/2} C_0 \quad (1)$$

where  $I_{pa}$  refers to the anodic peak current,  $n$  the electron transfer number,  $A$  the surface area of the electrode,  $D_R$  the diffusion coefficient,  $C_0$  the concentration of  $K_2Fe(CN)_6$  and  $v$  is the scan rate. For 1.0 mmol L<sup>-1</sup>

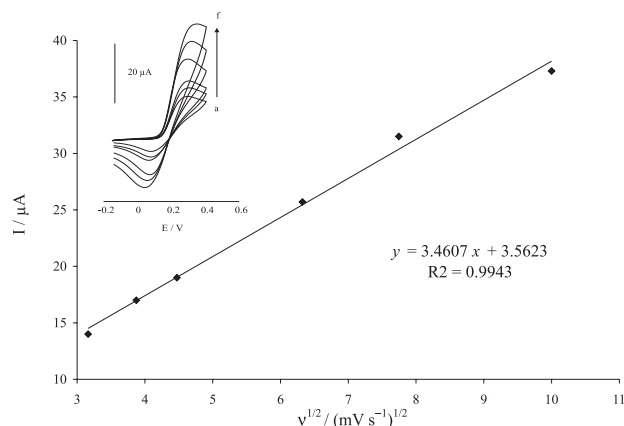


Figure 2. Plot of  $I_{pa}$  versus  $v^{1/2}$  for the oxidation of 500  $\mu\text{mol L}^{-1}$  3,4-DHCA at a surface of MWCNTPE. Inset: cyclic voltammograms at various scan rates, (a) 5; (b) 10; (c) 15; (d) 20; (e) 40 and (f) 100  $\text{mV s}^{-1}$  in 0.1 mol L<sup>-1</sup> PBS (pH 7.0).

$K_2Fe(CN)_6$  in 0.10 mol L<sup>-1</sup> KCl electrolyte with  $n = 1$  and  $D_R = 7.6 \times 10^{-6} \text{ cm}^2 \text{ s}^{-1}$  and from the slope of the  $I_{pa}$ - $v^{1/2}$  relation, the microscopic areas were calculated. The active surface areas were equal to 0.05 and 0.091  $\text{cm}^2$  for CPE and MWCNTPE, respectively. The result shows that the presence of MWCNTPE causes the increase of the active surface of the electrode.

#### Catalytic effect

Figure 3 depicts the cyclic voltammetric responses from the electrochemical oxidation of 500  $\mu\text{mol L}^{-1}$  CA at the MWCNTPE in the presence of 500  $\mu\text{mol L}^{-1}$  3,4-DHCA (curve c), CPE in the presence of 3,4-DHCA (curve b), MWCNTPE (without mediator) (curve d), and CPE (without mediator) (curve e).

As shown, the anodic peak potential for CA oxidation at the MWCNTPE in the presence of 3,4-DHCA (curve c)

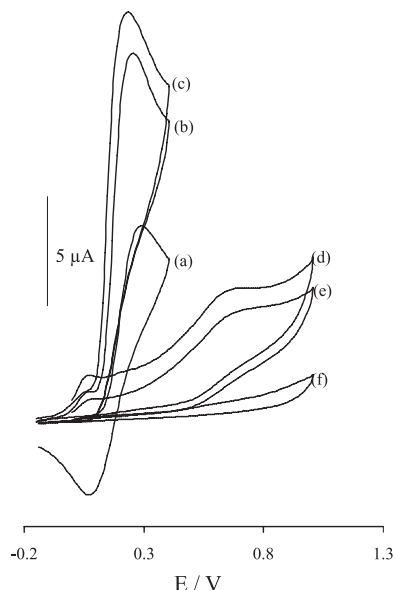
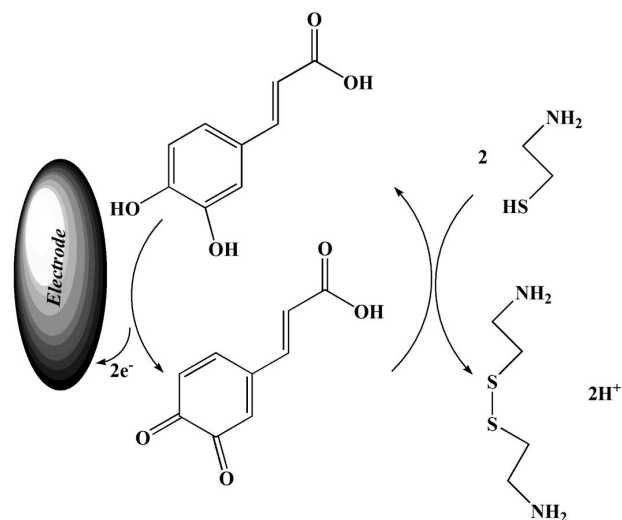


**Figure 3.** Cyclic voltammograms of (a)  $500 \mu\text{mol L}^{-1}$  3,4-DHCA at the surface of MWCNTPE in  $0.1 \text{ mol L}^{-1}$  PBS (pH 7.0), (b)  $500 \mu\text{mol L}^{-1}$  3,4-DHCA +  $500 \mu\text{mol L}^{-1}$  CA at the surface of carbon paste electrode, (c)  $500 \mu\text{mol L}^{-1}$  CA at the surface of MWCNTPE, (d)  $500 \mu\text{mol L}^{-1}$  3,4-DHCA +  $500 \mu\text{mol L}^{-1}$  CA at the surface of MWCNTPE, (e)  $500 \mu\text{mol L}^{-1}$  CA at the surface of carbon paste electrode, (f) for the buffer solution at the surface of unmodified electrode (carbon paste electrode); scan rate of  $20 \text{ mV s}^{-1}$ .

and CPE in the presence of 3,4-DHCA (curve b) was about  $0.217 \text{ mV}$ , while at the MWCNTPE (without mediator) (curve d), the peak potential was about  $620 \text{ mV}$ . At the unmodified CPE and without mediator, the peak potential was about  $670 \text{ mV}$  of CA (curve e) with lower oxidation current. From these results, it was concluded that the best electrocatalytic effect for CA oxidation was observed at the MWCNTPE in the presence of 3,4-DHCA (curve c). For example, results show that the peak potential of CA oxidation at the MWCNTPE in the presence of 3,4-DHCA (curve c) shifted by about  $403$  and  $453 \text{ mV}$  toward negative values when compared with that at the MWCNTPE and CPE without mediator (curve d and e), respectively.

Similarly, when comparing the oxidation of CA at the MWCNTPE (curve c) and CPE (curve b) in the presence of mediator, a dramatic enhancement of the anodic peak current at the MWCNTPE relative to that obtained at the CPE in the presence of mediator was observed. In other words, the data clearly show that the combination of multiwall carbon nanotubes and mediator definitely improve the characteristics of CA oxidation. The 3,4-DHCA at a surface of MWCNTPE, in  $0.1 \text{ mol L}^{-1}$  PBS (pH 7.0) and without CA in solution, exhibited a well-behaved redox reaction (curve a). The process corresponds to an EC' (catalytic) mechanism (see Scheme 1), where the electrochemically formed  $3,4\text{-DHCA}_{(\text{Ox})}$  reacts chemically with CA diffused toward the electrode surface, while the

simultaneous oxidation of the regenerated  $3,4\text{-DHCA}_{(\text{Red})}$  causes an increase in the anodic current. For the same reason, the cathodic current of the modified electrode is smaller in the presence of CA.



**Scheme 1.** Electrochemical mechanism for determination of CA at the surface of MWCNTPE in the presence of the mediator.

Since CA has a thiol moiety, it was anticipated that the oxidation of CA would be pH-dependent. In order to ascertain this, the voltammetric response of CA at a surface of MWCNTPE in presence of mediator was obtained in solutions with varying pH. Results show that the maximum value of the peak current appeared at pH 7.0, so this value was selected throughout the experiments (not shown).

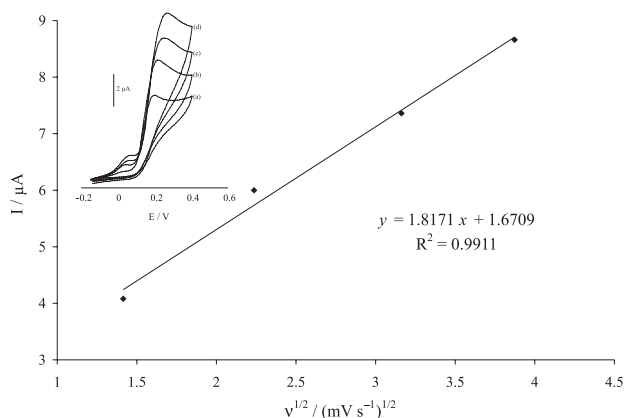


**Figure 4.** Plot of  $I_{pa}$  versus  $v^{1/2}$  for the oxidation of  $500 \mu\text{mol L}^{-1}$  CA in the presence  $500 \mu\text{mol L}^{-1}$  3,4-DHCA at the surface of MWCNTPE. Inset-Cyclic voltammograms of  $500 \mu\text{mol L}^{-1}$  CA in the presence of  $500 \mu\text{mol L}^{-1}$  3,4-DHCA at various scan rates: (a) 2, (b) 5, (c) 10 and (d)  $15 \text{ mV s}^{-1}$  in  $0.1 \text{ mol L}^{-1}$  buffer solution (pH 7.0).

The effects of scan rate ( $v$ ) on the oxidation current of CA were also examined (Figure 4). The peak current increased linearly with the increase of the square root of

scan rate that ranged from 2 to 15 mV s<sup>-1</sup> and it can be expressed as follows,

$$I_p = 1.8171 v^{1/2} + 1.6709 \quad (2)$$

( $r^2 = 0.9911$ ,  $I$  in  $\mu\text{A}$ ,  $v$  in  $\text{mV s}^{-1}$ )

This result shows that the electrode process is diffusion-controlled.

To obtain information about the rate-determining step, a Tafel plot was drawn, as derived from points in the Tafel region of the cyclic voltammogram (Figure 5).

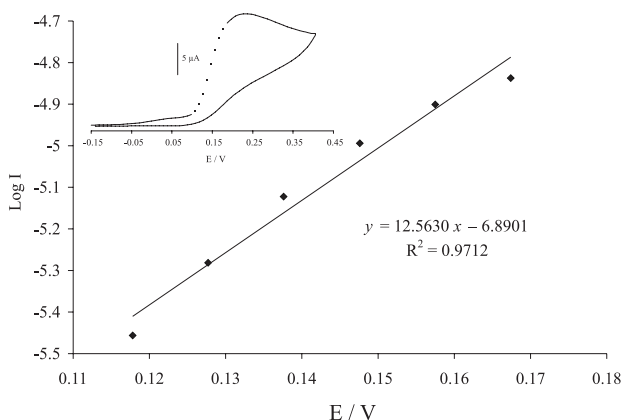


**Figure 5.** Tafel plot of 500  $\mu\text{mol L}^{-1}$  3,4-DHCA at the surface of MWCNTPE in 0.1 mol  $\text{L}^{-1}$  PBS (pH 7.0) at a scan rate of 20  $\text{mV s}^{-1}$  in the presence of 500  $\mu\text{mol L}^{-1}$  CA.

The slope of the Tafel plot was equal to  $n(1 - \alpha)F/(2.3RT)$ , which came up to 11.1563 V decade<sup>-1</sup>. Therefore, a value of  $\alpha$  equal to 0.26 was obtained.

In addition, the value of  $\alpha$  was calculated for the oxidation of CA at pH 7.0 for the MWCNTPE in both the absence and presence of mediator using the following equation,<sup>34,35</sup>

$$\alpha n_{\alpha} = 0.048/(E_p - E_{p/2}) \quad (3)$$

where  $E_{p/2}$  is the potential corresponding to  $I_{p/2}$ . The values for  $\alpha n_{\alpha}$  were found to be 0.18 and 0.34 at the surface of the MWCNTPE in the absence and presence of mediator, respectively. Those values show that the overpotential of CA oxidation is reduced at the surface of MWCNTPE in the presence of mediator, and also that the rate of electron transfer process is greatly enhanced. This phenomenon is, thus, confirmed by the larger  $I_{pa}$  values recorded during cyclic voltammetry at MWCNTPE in the presence of mediator.

Figure 6A shows the current-time curves of MWCNTPE in the presence of mediator by setting the electrode potential at 0.0 mV (first step) and 350 mV (second step) for

different CA concentrations. As can be seen, there is no net anodic current corresponding to the oxidation of the mediator in the presence of CA. On the other hand, the forward and backward potential step chronoamperometry for the mediator in the absence of CA shows symmetrical chronoamperogram with an equal charge consumed for the reduction and oxidation of the mediator at the surface of MWCNTPE (Figure 6B, a'). On the other hand, the charge value associated with forward chronoamperometry in the presence of CA is significantly greater than that observed for backward chronoamperometry (Figure 6B, b' and c').

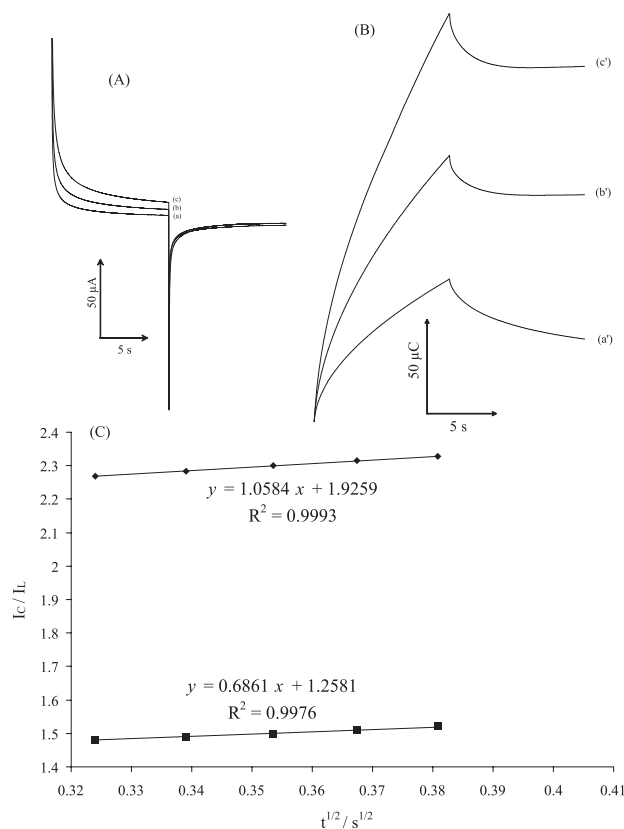


**Figure 6.** (A) Chronoamperograms obtained at the MWCNTPE in the absence (a) and in the presence of (b) 100 and (c) 200  $\mu\text{mol L}^{-1}$  CA in a buffer solution (pH 7.0). (B) The charge-time curves (a') for curve (a), (b') for curve (b), (c') for curve (c), (d') for curve (d) and (e') for curve (e). (C) Dependence of  $I_C/I_L$  on the  $t^{1/2}$  derived from the chronoamperogram data.

The rate constant for the chemical reaction between 3,4-DHCA and CA ( $k_h$ ) is determined according to the method of Galus,<sup>36</sup>

$$I_C/I_L = \pi^{1/2} \gamma^{1/2} = \pi^{1/2}(k_h t)^{1/2} \quad (4)$$

where  $I_C$  is the catalytic current of 3,4-DHCA in the presence of CA and  $I_L$  is the limiting current in the absence of CA. From the slope of  $I_C/I_L$  versus  $t^{1/2}$  for five different concentrations of CA, the average value of  $k_h$  was calculated

to be  $1.641 \times 10^3 \text{ mol}^{-1} \text{ L s}^{-1}$  (Figure 6C). This value of rate constant explains the sharp catalytic peak observed for the oxidation of glutathione (GSH) at the surface of MWCNTPE in the presence of mediator.

#### Stability and reproducibility

The repeatability and stability of MWCNTPE in the presence of mediator were investigated by linear sweep voltammetric measurements of  $10.0 \mu\text{mol L}^{-1}$  CA. The relative standard deviation (RSD in %) for seven successive assays was 1.8%. When using four different electrodes, the RSD for five measurements was 2.8%. When the electrode is stored in the laboratory, the modified electrode retains 98% of its initial response after a week and 95% after 30 days. These results indicate that MWCNTPE has a good stability and reproducibility, and could be used for CA analysis.

#### Dynamic range and limit of detection

Linear sweep voltammetry (LSV) was used for determination of CA. The LS voltammograms clearly showed two linear dynamic ranges that the plot of the peak current *versus* CA concentration was linear for  $0.25\text{-}2.5 \mu\text{mol L}^{-1}$  with a regression equation of  $I_p(\mu\text{A}) = 0.890 C_{\text{CA}} + 4.465$  ( $R^2 = 0.991$ ,  $n = 5$ ) (Figure 7A) and for  $3\text{-}400 \mu\text{mol L}^{-1}$  of CA, the regression equation was  $I_p(\mu\text{A}) = (0.034 C_{\text{CA}} + 6.720)$  ( $r^2 = 0.992$ ,  $n = 8$ ) (Figure 7B) where  $C$  is  $\mu\text{mol L}^{-1}$  concentration of CA and  $I_p$  is the peak current. According to

the method mentioned in Skoog *et al.*,<sup>37</sup> the lower detection limit,  $C_m$ , was obtained by using the equation  $C_m = 3s_b/m$ , where  $s_b$  is the standard deviation of the blank response ( $\mu\text{A}$ ) and  $m$  is the slope of the calibration plot. The data analysis presents the value of lower limit detection of CA to be  $0.09 \mu\text{mol L}^{-1}$ . The detection limit, linear dynamic range, and sensitivity to CA with MWCNTPE in the presence of mediator are comparable to, and even better than, those recently developed using voltammetric methods. Table 1 presents comparisons of the results obtained from the proposed method and those from electrochemical methods recently reported.

#### Interference study

In order to evaluate the selectivity of the proposed sensor for the determination of CA, the influence of various foreign species on the determination of  $5.0 \mu\text{mol L}^{-1}$  CA was investigated. The tolerance limit was taken as the maximum concentration of the foreign substances, which caused an approximately  $\pm 5\%$  relative error in the determination.

The results after the experiments revealed that neither 1000-fold of  $\text{NO}_3^-$ ,  $\text{ClO}_4^-$ ,  $\text{SO}_4^{2-}$ ,  $\text{F}^-$ , glucose, sucrose, lactose, fructose, glycine, urea, histidine,  $\text{SCN}^-$ , methionine, alanine, and phenylalanine; nor 600-fold of tryptophan, thiourea, and tyrosine; nor 200-fold of uric acid and nor saturation of starch solution affected the selectivity. However, more than 3-fold of cysteine and ascorbic acid

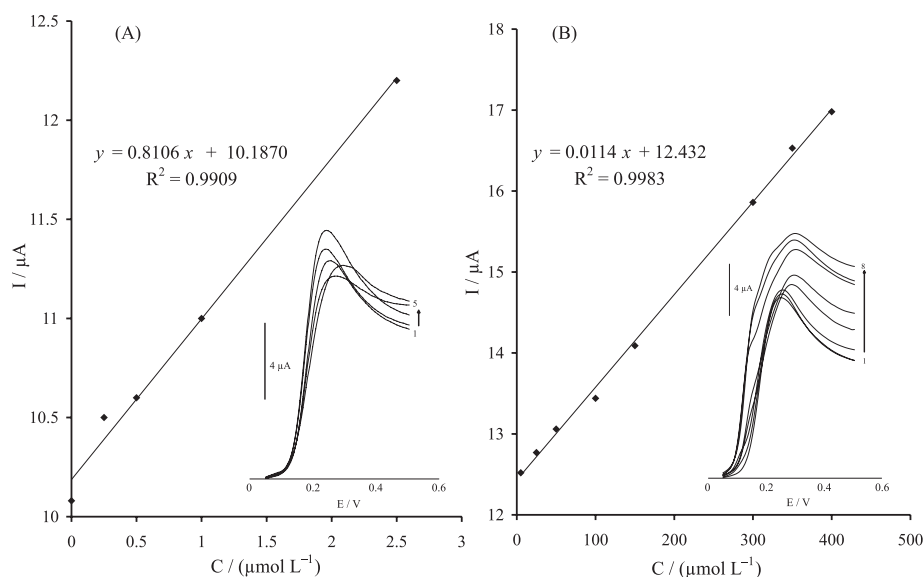


**Figure 7.** (A) Plots of the electrocatalytic peak current as a function of CA concentration in the range of  $0.25\text{-}2.5 \mu\text{mol L}^{-1}$ . Inset: modified electrode LSVs in  $0.1 \text{ mol L}^{-1}$  PBS (pH 7.0) containing different concentrations of CA. From inner to outer (1-5) correspond to  $0.0, 0.25, 0.5, 1.0$  and  $2.5 \mu\text{mol L}^{-1}$  of CA. (B) The plots of the electrocatalytic peak current as a function of CA concentration in the range of  $5.0\text{-}400.0 \mu\text{mol L}^{-1}$ . Inset: modified electrode LSVs in  $0.1 \text{ mol L}^{-1}$  PBS (pH 7.0) containing different concentrations of CA. From inner to outer (1-8) correspond to  $5.0, 25.0, 50.0, 100.0, 150.0, 300.0, 350.0$  and  $400.0 \mu\text{mol L}^{-1}$  of CA.

**Table 1.** Comparison of the efficiency of some electrochemical methods in the determination of CA

Electrode	Method	LOD / ( $\mu\text{mol L}^{-1}$ )	LOQ / ( $\mu\text{mol L}^{-1}$ )	Sensitivity $\mu\text{A} / (\mu\text{mol L}^{-1})$	Reference
SWCNT-Nq/GCE <sup>a</sup>	DPV <sup>b</sup>	3.0	5.0-270	0.058	11
PDMA/FMCPE <sup>c</sup>	CV <sup>d</sup>	79.7	80-1140	–	12
Nq/Au <sup>e</sup>	DPV	5.2	8.0-550	0.015	13
<i>p</i> -APMCNTPE <sup>f</sup>	DPV	0.15	0.5-300	0.243	14
FMCNTPE <sup>g</sup>	DPV	0.3	0.7-200	0.352	38
VFMWCNTPE <sup>h</sup>	SWV	0.05	0.09-500	0.3406	39
MWCNTPE	LSV	0.09	0.25-400	0.890	this work

<sup>a</sup>Single-wall carbon nanotube 1,2-naphthoquinone-4-sulfonic acid modified glassy carbon electrode; <sup>b</sup>differential pulse voltammetry; <sup>c</sup>poly-N,N-dimethylaniline/ferrocyanide film modified carbon paste electrode; <sup>d</sup>cyclic voltammetry; <sup>e</sup>1,2-naphthoquinone-4-sulfonic acid sodium (Nq)-modified gold electrode; <sup>f</sup>carbon nanotube paste electrode modified with *p*-aminophenol; <sup>g</sup>ferrocene-modified carbon nanotube paste electrode; <sup>h</sup>vinylferrocene-modified carbon nanotube paste electrode; LOD: Limit of determination; LOQ: limit of qualification.

**Table 2.** Determination of CA in real samples (n = 3)

Sample	Added / ( $\mu\text{mol L}^{-1}$ )	Expected / ( $\mu\text{mol L}^{-1}$ )	Found / ( $\mu\text{mol L}^{-1}$ )	Found <sup>14</sup> / ( $\mu\text{mol L}^{-1}$ )	F <sub>ex</sub>	F <sub>tab</sub>	t <sub>ex</sub>	t <sub>tab</sub>
Capsule	–	5.00	5.58±0.62	5.90±0.7591	8.5	19	2.2	3.8
	5.00	10.00	10.42±0.55	10.83±0.90	7.0	19	2.0	3.8
	10.00	20.00	20.34±0.41	20.63±0.70	5.5	19	1.7	3.8
Urine <sup>a</sup>	–	–	< LOD	< LOD	–	–	–	–
	40.00	40.00	40.71±0.85	41.00±1.01	8.0	19	2.1	3.8
	10.00	50.00	50.78±0.80	50.88±0.92	8.3	19	2.1	3.8
Urine <sup>b</sup>	–	–	6.45±0.50	6.85±0.68	5.8	19	1.8	3.8

<sup>a</sup>Healthy person; <sup>b</sup>urine samples of patients undergoing treatment with CA.

affect the selectivity. Those results confirm the suitable selectivity of the proposed sensor for CA determination.

#### Determination of CA in real samples

In order to demonstrate the ability of the modified electrode to determine CA in real samples, these compounds were determined in capsule and urine samples. The results are presented in Table 2. Clearly, modified electrode is capable of voltammetric determination of CA with high selectivity and good reproducibility.

#### Conclusions

This work demonstrates the construction of a chemically modified carbon paste electrode by incorporating multiwall carbon nanotubes as a suitable electrochemical sensor in the presence of 3,4-DHCA as a mediator for CA determination at trace level. The new voltammetric method for the determination of CA is very rapid (less than 1 min per sample solution), reproducible, selective and sensitive, and can be used for real sample analysis. The results show that the oxidation of CA is

catalyzed at pH 7.0, whereas the peak potential of CA is shifted by 403 mV to a less positive potential at the surface of the MWCNTPE in the presence of mediator. The proposed method is a selective, simple and precise method for voltammetric determination of CA in real samples such as drug and urine, as low as 0.09  $\mu\text{mol L}^{-1}$  CA. In addition, the kinetic parameters of the system have been calculated from the experimental results.

#### Acknowledgements

The authors wish to thank Shahreza and Majlesi Branch, Islamic Azad University, for their support.

#### References

- Gahl, W. A.; *Eur. J. Pediatr.* **2003**, *162*, 38.
- Gahl, W. A.; Bashan, N.; Tietze, F.; Bernadini, I.; Schulman, J. D.; *Science* **1982**, *217*, 1263.
- Gahl, W. A.; Thoene, J. G.; Schneider, J. A.; Scriver, C. R.; Beaudet, A. L.; Sly, W. S.; Valle, D., eds. *The Metabolic and Molecular Basis of Inherited Disease*, 8<sup>th</sup> ed.; McGraw-Hill: New York, NY, USA, 2001,

4. Thoene, J. G.; *J. Inherit. Metab. Dis.* **1995**, *18*, 380.
5. Lochman, P.; Adam, T.; Fredecky, D.; Hlidkova, E.; Stopover, Z.; *Electrophoresis* **2003**, *24*, 1200.
6. Stachowicz, M.; Lehmann, B.; Tibi, A.; Prognon, P.; Daurat, V.; Pradeau, D.; *J. Pharm. Biomed. Anal.* **1998**, *17*, 767.
7. Kataoka, H.; Lmamura, Y.; Tanaka, H.; Makita, M.; *J. Pharm. Biomed. Anal.* **1993**, *11*, 963.
8. Kataoka, H.; Tanaka, H.; Makita, M.; *J Chromatogr B Biomed Appl.* **1994**, *657*, 9.
9. Jonas, A. J.; Schneider, J. A.; *Anal. Biochem.* **1981**, *114*, 429.
10. Kataoka, H.; Tanaka, H.; Makita, M.; *J. Chromatogr., B* **1994**, *657*, 9.
11. Hsiung, M.; Yeo, Y.Y.; Itiaba, K.; Crawhall, J. C.; *Biochem. Med.* **1978**, *19*, 305.
12. Raoof, J. B.; Ojani, R.; Chekin, F.; *J. Mater. Sci.* **2009**, *44*, 2688.
13. Ojani, R.; Raoof, J. B.; Zarei, E.; *Electroanalysis* **2009**, *21*, 1189.
14. Ensafi, A. A.; Karimi-Maleh, H.; *Electroanalysis* **2010**, *22*, 2558.
15. Saraji, M.; Bidgoli, A. A. H.; *J. Chromatogr, A* **2009**, *1216*, 1059.
16. Saraji, M.; Bidgoli, A. A. H.; *Anal. Bioanal. Chem.* **2009**, *397*, 3107.
17. Saraji, M.; Khalili Boroujeni, M.; Bidgoli, A. A. H.; *Anal. Bioanal. Chem.* **2011**, *400*, 2149.
18. Khalilzadeh, M. A.; Karimi-Maleh, H.; Amiri, A.; Gholami, F.; Motaghd mazhabi, R.; *Chin. Chem. Lett.* **2010**, *21*, 1467.
19. Ensafi, A. A.; Taei, M.; Khayamian, T.; Karimi-Maleh, H.; Hasanpour, F.; *J. Solid State Electrochem.* **2010**, *14*, 1415.
20. Beitollah, H.; Goodarzian, M.; Khalilzadeh, M. A.; Karimi-Maleh, H.; Hassanzadeh, M.; Tajbakhsh, M.; *J. Mol. Liq.* **2012**, *173*, 137.
21. Beitollahi, H.; Karimi-Maleh, H.; Khabazzadeh, H.; *Anal. Chem.* **2008**, *80*, 9848.
22. Pumera, M.; *Chem. Eur. J.* **2009**, *15*, 4970.
23. Crevilln, A. G.; Avila, M.; Pumera, M.; Gonzalez, M. C.; Escarpa, A.; *Anal. Chem.* **2007**, *79*, 7408.
24. Wei, B.; Wang, J.; Chen, Z.; Chen, G.; *Chem. Eur. J.* **2008**, *14*, 9779.
25. Pumera, M.; Llopis, X.; Merkoci, A.; Alegret, S.; *Microchim. Acta* **2006**, *152*, 261.
26. Nugent, J. M.; Santhanam, K. S. V.; Rubio, A.; Ajayan, P. M.; *Nano Lett.* **2001**, *1*, 87.
27. Musameh, M.; Wang, J.; Merkoci, A.; Lin. Y.; *Electrochem. Commun.* **2002**, *4*, 743.
28. Pumera, M.; Merkoci, A.; Alegret, S.; *Sens. Actuators, B* **2006**, *113*, 617.
29. Ensafi, A. A.; Karimi-Maleh, H.; *J. Electroanal. Chem.* **2010**, *640*, 75.
30. Ensafi, A. A.; Karimi-Maleh, H.; Mallakpour, S.; Hatami, M.; *Sens. Actuators, B* **2011**, *155*, 464.
31. Afzali, D.; Karimi-Maleh, H.; Khalilzadeh, M.A.; *Environ. Chem. Lett.* **2011**, *9*, 375.
32. Ensafi, A. A.; Karimi-Maleh, H.; Mallakpour, S.; Rezaei, B.; *Colloid Surf., B* **2011**, *87*, 480.
33. Akhgar, M. R.; Beitollahi, H.; Salari, M.; Karimi-Maleh, H.; Zamani, H.; *Anal. Methods* **2012**, *4*, 259.
34. Raoof, J. B.; Ojani, R.; Karimi-Maleh, H.; *Electroanalysis* **2008**, *20*, 1259.
35. Karimi-Maleh, H.; Ensafi, A. A.; Ensafi, H. R.; *J. Braz. Chem. Soc.* **2009**, *20*, 880.
36. Galus, Z.; *Fundamentals of Electrochemical Analysis*; Ellis Horwood: New York, NY, USA, 1976.
37. Skoog, D. A.; Holler, F. J.; Nieman, T. A.; *Principles of Instrumental Analysis*, 5<sup>th</sup> ed.; Harcourt Brace: Philadelphia, USA, 1998.
38. Taherkhani, A.; Karimi-Maleh, H.; Ensafi, A. A.; Beitollahi, H.; Hosseini, A.; Khalilzadeh, M.A.; Bagheri, H.; *Chin. Chem. Lett.* **2012**, *23*, 237.
39. Keyvanfard, M.; Ensafi, A. A.; Karimi-Maleh, H.; *J. Solid State Electrochem.* **2012**, *16*, 2949.

Submitted: January 21, 2012

Published online: February 7, 2013